


Article

Electrically Conductive Silicate Composite for Protection against Electrocorrosion

Andrii Plugin¹, Teresa Rucińska² , Olga Borziak^{1,2,*} , Oleksii Pluhin¹ and Vitalii Zhuravel¹

¹ Faculty of Construction, Ukrainian State University of Railway Transport, Feuerbach sq. 7, 61050 Kharkiv, Ukraine

² Faculty of Civil and Environmental Engineering, West Pomeranian University of Technology in Szczecin, al. Piastów 50A, 70-311 Szczecin, Poland

* Correspondence: oborziak@zut.edu.pl

Abstract: This article presents the results of a study on the development of an anti-corrosion plaster composite based on water glass with increased electrical conductivity. Known acid-resistant quartz-fluorosilicate composites containing liquid sodium silicate, sodium fluorosilicate and acid-resistant high-silica filler in the form of quartz, andesite or diabase powder were chosen as the prototype. The low water resistance and low adhesion to Portland cement concrete of these composites limits their application. By adding granulated blast-furnace slag to the composite, it was possible to increase the water resistance of the solution and its adhesion to concrete. The addition of graphite filler to the composite made it possible to increase the electrical conductivity. This made it possible to obtain not only a corrosion-resistant (to chemical and physico-chemical corrosion) composite, but also to use it as a grounded protective screen to drain leakage currents from the structure, thus protecting it from both corrosion and electrocorrosion destruction.

Keywords: silicate composite; electrocorrosion; water glass; mineral binder



Citation: Plugin, A.; Rucińska, T.; Borziak, O.; Pluhin, O.; Zhuravel, V. Electrically Conductive Silicate Composite for Protection against Electrocorrosion. *Minerals* **2023**, *13*, 610. <https://doi.org/10.3390/min13050610>

Academic Editor: Kenneth N. Han

Received: 15 March 2023

Revised: 16 April 2023

Accepted: 26 April 2023

Published: 27 April 2023



Copyright: © 2023 by the authors. Licensee MDPI, Basel, Switzerland. This article is an open access article distributed under the terms and conditions of the Creative Commons Attribution (CC BY) license (<https://creativecommons.org/licenses/by/4.0/>).

1. Introduction

Electrocorrosion of construction from leakage currents from direct current sources, mainly electrified transport, causes significant damage worldwide. The most reliable methods of protection against it are electrochemical, incl. drainage of electrical currents in various ways. These methods involve the use of grounding devices, electrically conductive metal screens, etc. However, metals are expensive, and devices made of them quickly corrode themselves, instead of the structure. It is promising to develop electrically conductive composites based on mineral binders for the development of electrocorrosion protection devices using plastering and painting methods [1–3].

Electrically conductive composites based on mineral binders are widely used in modern construction. These composites, incl. concretes, are used for the practice of monitoring deformation changes in structures. The application of these composites as strain sensors is due to a change in the electrical resistivity with strain. In work [4], concrete with nano-carbon black and carbon fiber, which were added as electrically conductive materials, was researched. The effects of the beam damage degree on the fractional change in resistance were investigated. It was also concluded that the electrically conductive addition used had little effect on the strength of the concrete. In reference [5], properties of cement composites with the addition of carbon fibers and carbon nanofibers were studied. The possibility of using these composites as strain sensors in elastic sensing condition testing was evaluated. In work [6], steel fibers were used as electrically conductive elements, and silica fume was used to improve strength and accelerate material dispersion in cement composites. According to the research, silica fume contributes indirectly to conductivity by permitting the dispersion of conductive materials. The effectiveness of the simultaneous use of steel fiber and silica fume was proven in the work—the resistivity of the composite was reduced by

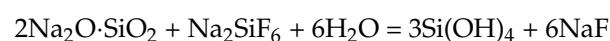
94%. The papers [7,8], etc., confirmed the effectiveness of the use of electrically conductive concrete in the heating system of pavements and for bridge deck deicing. In work [7], steel fibers and shaving were added to the concrete as conductive materials. In reference [8], the influence of a variety of factors on the electrical and mechanical characteristics of electrically conductive concrete was investigated, while carbon fiber in different size classes was used as an electrically conductive constituent, methyl cellulose was used as a fiber dispersive agent and corrosion inhibitor admixtures were used as conductivity-enhancing agents. It is also known about the use of electrically conductive composites as shielding elements from electromagnetic interference; for example, in [9], to improve the characteristics of electromagnetic shielding of concrete, graphite powder, carbon black and steel fibers were introduced to its composite. In works [10,11], the effectiveness of the use of cement conductive anodes for the application of cathodic protection to control corrosion in reinforced concrete structures was evaluated and proved.

The main components of such electrically conductive composites are mineral binders, aggregates of varying degrees of dispersion, water, electrically conductive additive and chemical admixtures [12]. Such composites use such mineral binders as Portland cement [13,14] or alkaline binders [15–17].

Electrically conductive composites based on Portland cement are characterized by poor fluidity [18], their consumption per 1 m² of structure is high and their use for structures with still-intact concrete requires a feasibility study. The creation of a composite with improved fluidity and which could be applied in a thin layer could possibly be based on sodium silicates. An analysis of works [15–17,19,20] and other studies of alkaline binders suggested the possibility of creating an electrically conductive silicate composite based on water glass—sodium silicate for screen protection of structures that do not require restoration of the bearing capacity and repair of the surface.

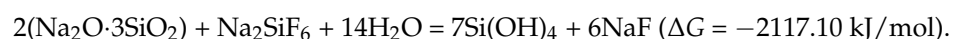
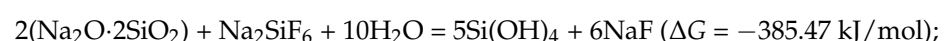
2. Theoretical Justifications for the Development of the Composite of the Electrically Conductive Silicate Composite

Silicate composites based on water glass and mineral fillers are used more often for corrosion protection in acidic media [21]. Usually, acid-resistant fillers—diabase, andesite, etc.—and a hardener—sodium fluorosilicate—are used. Sodium silicates $n\text{Na}_2\text{O}\cdot m\text{SiO}_2$ interact with sodium fluorosilicate Na_2SiF_6 to form a gel of silicic acid $\text{Si}(\text{OH})_4$, which provides binding properties due to coagulation [21]:



However, such composites have insufficient water resistance (softening coefficient), no more than 0.2, and it was proposed in [1,3,21] to increase it via the introduction of ground basic blast-furnace granulated slag instead of part or all of sodium fluorosilicate. By analogy with slag–alkali binders [22,23], the interaction of its silicate and aluminates minerals and glass with sodium silicate causes the formation of a certain amount of zeolite-like calcium, alkali and alkaline earth aluminosilicates, which provide an increase in water resistance.

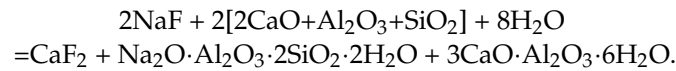
Theoretical studies have been carried out to improve the water resistance of silicate composites by introducing ground blast-furnace granulated slag, in particular, thermodynamic calculations [3]. Based on the negative values of the Gibbs free energy of the reactions, it was concluded that in the case of curing of sodium silicates with sodium fluorosilicate, the products of their interaction are orthosilicic acid gel $\text{Si}(\text{OH})_4$ and sodium fluoride:



According to the research of Professor P. Krivenko [23], sodium fluoride NaF, when interacting with minerals of blast-furnace slag of the gehlenite type C_2AS , forms zeolite-like calcium-sodium hydroaluminosilicates (hydronepheline NAS_2H_2 , calcium hydroaluminate

C_3AH_6 , C_2AH_8), calcium hydrosilicates $C_2S_3H_{2.5}$, C_6S_6H and slightly soluble (0.016 g/L) calcium fluoride CaF.

Thermodynamic calculations were performed to establish the possibility of the formation of hydronepheline NAS_2H_2 , calcium hydroaluminat C_3AH_6 and calcium fluoride CaF_2 due to the interaction of slag with sodium fluoride NaF according to the scheme:



For thermodynamic calculations for slag, the conditional compound $[2CaO + Al_2O_3 + SiO_2]$ was adopted, for which the value $\Delta G = -3808.31$ kJ/mol was taken as for C_2AS according to [24], and for which it is possible to construct stoichiometric equations. The value of the Gibbs free energy ΔG , the formation of compounds from elements, is taken from the data of [24].

$$\Delta G = \Delta G_{NAS_2H_2} + \Delta G_{C_3AH_6} + \Delta G_{CaF_2} - 2\Delta G_{C_2AS} - \Delta G_{NaF} - 8\Delta G_{H_2O} \\ = -4463.13 + (5017.46) + (-1113.44) - 2 \cdot (-3808.31) - (-542.57) - 8 \cdot (-237.34) \\ = -536.14 \text{ kJ/mol}$$

The results of calculations of the Gibbs free energy of this and other possible reactions of the interaction of this conditional compound with various alkaline components are given in Table 1.

Table 1. Gibbs free energy ΔG of reactions of the interaction of gehlenite (in terms of one molecule) with alkaline components to form analcime NAS_4H_2 and hydronepheline NAS_2H_2 .

Alkaline Component	Gibbs Free Energy ΔG , kcal/mol, of Reactions of the Interaction of Main and Additional Products			
	Hydronepheline NAS_2H_2		Analcime NAS_4H_2	
	ΔG	Additional Products	ΔG	Additional Products
$NaO \cdot 2SiO_2$	-33.172	$C_2S_3H_{2.5}$; $Ca(OH)_2$	-14.792	C_2AH_8 ; $Ca(OH)_2$
$NaO \cdot 3SiO_2$	-949.120	C_6S_6H	27.331	$Ca(OH)_2$
Na_2SiF_6	-208.490	C_3AH_6 ; $CaSiF_6$	-29.383	C_2AH_8 ; $CaSiF_6$; $Ca(OH)_2$
NaF	-268.07	C_3AH_6 ; CaF_2	17.019	C_2AH_8 ; CaF_2 ; $Ca(OH)_2$

The model of a dispersed system, which properties determine the surface phenomena and electrical surface properties of the particles of the dispersed phase and the contacts between them, is of great importance for the analysis of stability under operating conditions of composite materials based on mineral binders. Electric surface charges are quantitatively characterized by the electrosurface potential ψ , V. In [25–27], a method for determining the absolute and equilibrium electrosurface potentials of substances using electrochemical and energy calculation and experimental methods was developed. Using this method, the electrical surface potentials of the particles of the formed compounds were determined.

Absolute electrosurface potentials ψ_{XYZ}^0 and equilibrium electrosurface potentials ψ_{XYZ}^E were calculated using the following:

$$\psi_{XYZ}^0 = -\frac{x\psi_X^0 + y\psi_Y^0 + z\psi_Z^0}{x + y + z} \quad (1)$$

$$\psi_{XYZ}^E = \psi_{XYZ}^0 - 0.059\text{pH} \quad (2)$$

where ψ_{XYZ}^0 , ψ_{XYZ}^E , respectively, are the absolute and equilibrium electrosurface potentials of the compound $X_xY_yZ_z$; ψ_X^0 , ψ_Y^0 and ψ_Z^0 are the absolute electrosurface potentials of simple substances that make up the compound $X_xY_yZ_z$ (Table 2). For the pore electrolyte of orthosilicic acid gel $\text{Si}(\text{OH})_4$, the pH value is taken equal to seven.

Table 2. Absolute electrosurface potentials ψ^0 of simple substances included in the composite of the studied compounds [26,27].

Element	Ca	Na	Al	Si	H	O	F
ψ^0, B	−4.20	−4.04	−2.99	−1.23	−1.2	+1.44	+4.89

Absolute electrosurface potentials ψ_{XYZ}^0 and equilibrium electrosurface potentials ψ_{XYZ}^E of orthosilicic acid gel $\text{Si}(\text{OH})_4$, hydronepheline NAS_2H_2 , calcium hydroaluminat C_3AH_6 are equal to, respectively:

$$\psi_{\text{Si}(\text{OH})_4}^0 = -\frac{\psi_{\text{Si}}^0 + 4\psi_{\text{O}}^0 + 4\psi_{\text{H}}^0}{1 + 4 + 4} = -\frac{-1.23 + 4 \cdot 1.44 + 4 \cdot (-1.2)}{1 + 4 + 4} = 0.03 \text{ V} \tag{3}$$

$$\psi_{\text{Si}(\text{OH})_4}^E = \psi_{\text{Si}(\text{OH})_4}^0 - 0.059\text{pH} = 0.03 - 0.059 \cdot 7 = -0.383 \text{ V} \tag{4}$$

$$\begin{aligned} \psi_{\text{NAS}_2\text{H}_2}^0 &= -\frac{2\psi_{\text{Na}}^0 + 2\psi_{\text{Al}}^0 + 2\psi_{\text{Si}}^0 + 4\psi_{\text{H}}^0 + 10\psi_{\text{O}}^0}{2+2+2+4+10} \\ &= -\frac{2 \cdot (-4.04) + 2 \cdot (-2.99) + 2 \cdot (-1.23) + 4 \cdot (-1.2) + 10 \cdot 1.44}{2+2+2+4+10} = 0.346 \text{ V} \end{aligned} \tag{5}$$

$$\psi_{\text{NAS}_2\text{H}_2}^E = \psi_{\text{NAS}_2\text{H}_2}^0 - 0.059\text{pH} = 0.346 - 0.059 \cdot 7 = -0.067 \text{ V} \tag{6}$$

$$\begin{aligned} \psi_{\text{C}_3\text{AH}_6}^0 &= -\frac{3\psi_{\text{Ca}}^0 + 2\psi_{\text{Al}}^0 + 12\psi_{\text{H}}^0 + 12\psi_{\text{O}}^0}{3+2+12+12} \\ &= -\frac{3 \cdot (-4.2) + 2 \cdot (-2.99) + 12 \cdot (-1.2) + 12 \cdot 1.44}{3+2+12+12} = 0.541 \text{ V} \end{aligned} \tag{7}$$

$$\psi_{\text{C}_3\text{AH}_6}^E = \psi_{\text{C}_3\text{AH}_6}^0 - 0.059\text{pH} = 0.541 - 0.059 \cdot 7 = 0.128 \text{ V} \tag{8}$$

The electrosurface potentials of sodium and calcium fluoride (NaF and CaF_2) were calculated in a similar way. The calculation results are summarized in Table 3.

Table 3. The electrical surface potentials of the products of the interaction of sodium silicate, sodium fluorosilicate and gehlenite.

Compound		Electrical Surface Potentials, V	
Name, Designation	Formula	Absolute ψ_{XYZ}^0	Equilibrium ψ_{XYZ}^E
orthosilicic acid	$\text{Si}(\text{OH})_4$	+0.03	−0.383
sodium fluoride	NaF	−0.425	−0.838
hydronepheline NAS_2H_2	$\text{Na}_2\text{O} \cdot \text{Al}_2\text{O}_3 \cdot 2\text{SiO}_2 \cdot 2\text{H}_2\text{O}$	+0.346	−0.067
calcium hydroaluminat C_3AH_6	$3\text{CaO} \cdot \text{Al}_2\text{O}_3 \cdot 6\text{H}_2\text{O}$	+0.541	+0.128
calcium fluoride	CaF_2	+1.86	+1.447

An analysis of the structure of the composites under consideration was carried out, taking into account their electrosurface properties. The main components of this structure are particles of orthosilicic acid gel. According to [28], gel particles are rounded particles ranging in size from 2–3 to 15 nm, sometimes up to 60 nm. Calcium hydroaluminat C_3AH_6 is usually represented by hexagonal crystals ranging in size from 50 nm to 500 nm, Figure 1. Fluorite CaF_2 crystals have cubic, octahedral and cuboctahedral shapes, and their sizes

under compressed growth conditions are apparently comparable to the sizes of orthosilicic acid gel particles and calcium hydroaluminate C_3AH_6 .

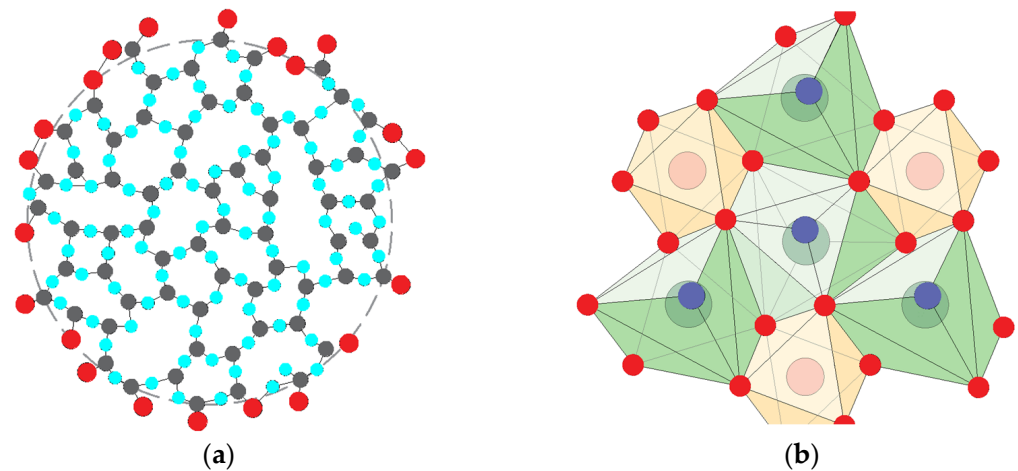


Figure 1. Structural representations of the orthosilicic acid gel $Si(OH)_4$ (a) and the calcium hydroaluminate C_3AH_6 (b) with silicon atoms in grey, oxygen atoms in light blue, hydroxyl groups in red, water molecules in dark blue, Ca polyhedra in light green and Al octahedra in dark green.

The microstructure of an artificial stone of sodium silicate cured with sodium silicon fluoride can be represented by the diagram in Figure 2a. Table 3 shows that $Si(OH)_4$ and NaF particles have a negative surface charge and form only electro-homogeneous contacts with each other (between particles with similarly charged surfaces through electrical double layers, Figure 2a), which, under dry conditions, due to high concentrations of pore electrolyte NaF, have high strength, but are not water resistant.

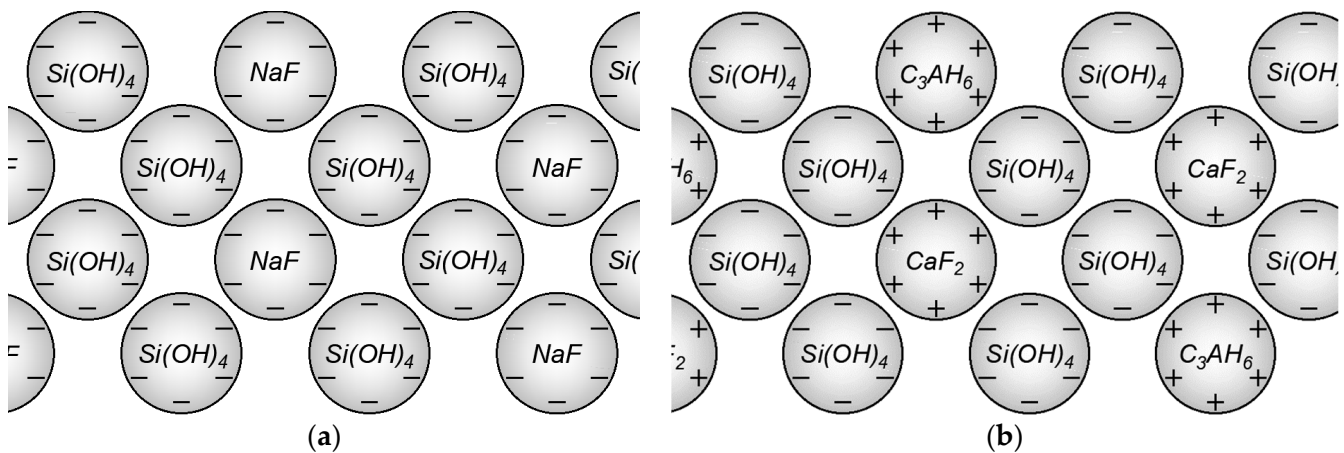


Figure 2. Schemes for the theoretical justification for the development of an electrically conductive silicate composite: (a) a scheme of the structure of a composite obtained as a result of the interaction of sodium silicate and sodium fluorosilicate without additives; (b) the same with the addition of blast-furnace granulated slag. All particles are shown the same size conventionally.

Hydronepheline particles also have a negative surface charge, while particles of calcium hydroaluminate C_3AH_6 and calcium fluoride CaF_2 have a positive surface charge. This suggests that the increase in the water resistance of an artificial stone of sodium silicate cured with sodium silicon fluoride, due to the addition of ground blast-furnace granulated slag, is provided not by the formation of zeolite-like hydroaluminosilicates according to [21], but by the formation of calcium hydroaluminate. In this case, electroheteroge-

neous contacts are formed between the particles of the gel of orthosilicic acid $\text{Si}(\text{OH})_4$ and calcium hydroaluminate.

Electrically conductive additives are the main components that form the electrical conductivity due to the formation of a continuous network in the composite matrix [29–31]. Electrically conductive additives can consist of a single material [32,33] or a mixture of different materials with high electrical conductivity [4,32]. An analysis of preliminary studies made it possible to identify the additive of finely dispersed graphite as the most effective one [32,34]; this additive has a relatively low cost and the best electrical properties (impedance). However, the issues of the interaction of carbon-graphite fillers with a silicate composite based on water glass and the effect on its properties have not been studied.

3. Materials and Methods

For the production of electrically conductive composites, a sodium silicate solution (water glass—Wg) with a silicate modulus of 2.7 was used, the hardener was sodium fluoro-silicate Na_2SiF_6 and the superplasticizer additive was sulfonated naphthalene formaldehyde. The combined filler consisted of blast-furnace granulated ground slag (S) from the Mariupol Metallurgical Plant—the chemical composite of slag is given in Table 4—and an electrically conductive fine graphite powder (G) of the lubricating grade GS-1—the properties are given in Table 5.

Table 4. The chemical composite of slag.

Oxide Compound	MgO	Al ₂ O ₃	SiO ₂	SO ₃	CaO	MnO	FeO	TiO ₂
Content (%wt.)	14.36	7.51	31.23	2.2	31.75	2.2	1.5	0.34

Table 5. The properties of graphite powder of the grade GS-1.

Properties	Value
Ash content	0.5%
Mass fraction of the copper	0.5%
Mass fraction of volatile substances	0.5%
Mass fraction of photo-reagents	0.5%
pH value	6.0–8.2

The mix designs were made to determine the effect of the content of the graphite powder additive on the electrical conductivity. In the composition, the graphite content varied from 0 to 4, and the content of liquid glass from 0.75 to 10 of the slag content by weight. Three batches were prepared with each mix design. From each batch, $40 \times 40 \times 160$ mm beam specimens were prepared for average density, water absorption W_m , bending and compressive strength f and coefficient of water resistance (softening) of K_{wr} measurements. The samples were tested after 28 days of natural hardening by standard (traditional) methods.

To determine the electrical properties, the studied composite was applied to the surface of samples of beams with a size of $40 \times 40 \times 160$ mm from a cement-sand mortar with a composite of 1:3 with water-to-cement ratio $W/C = 0.3$. Electrical resistivity ρ , $\Omega \times m$ and electrical conductivity σ , S/m of the coating from the studied composite were determined by the electrical resistance R , Ω . The electrical resistance was determined by measuring the voltage U , V and the current strength I , A in the measurement circuit (or directly). The applied electrodes used in research are stainless steel plates. The electrodes are applied to the coating through pads made of non-woven synthetic material 1.5–2 mm thick and impregnated with a saturated solution of copper sulphate. Voltage U and current I were measured using Sanwa PC500/510 digital multimeters, which allow measuring current, voltage, electrical resistance and capacitance and transmit their values to a PC that records them in real time.

The composite of hydration products and the nature of their interaction with an electrically conductive filler were studied using physicochemical methods of X-ray phase

analysis (using a DRON-3 X-ray diffractometer), analysis of infrared absorption spectra (Bruker Alpha IR-Fourier spectrometer) and a scanning electron microscope (SEM JEOL JSM-6390LV with energy dispersive spectrometer AZtechEnergy X-maxn50).

4. Results

In the development of research [20], experimental studies of the electrical, hydrophysical and physico-mechanical properties of the electrically conductive silicate composite were carried out depending on the relative content of graphite filler, sodium silicate and other composite indicators. The most important of the obtained dependencies are shown in Figure 3. Figure 3 shows that for silicate composites with graphite filler, the electrophysical characteristics are in antagonism with hydrophysical and physico-mechanical properties; therefore, the development of their formulations should be carried out by methods of compromise optimization.

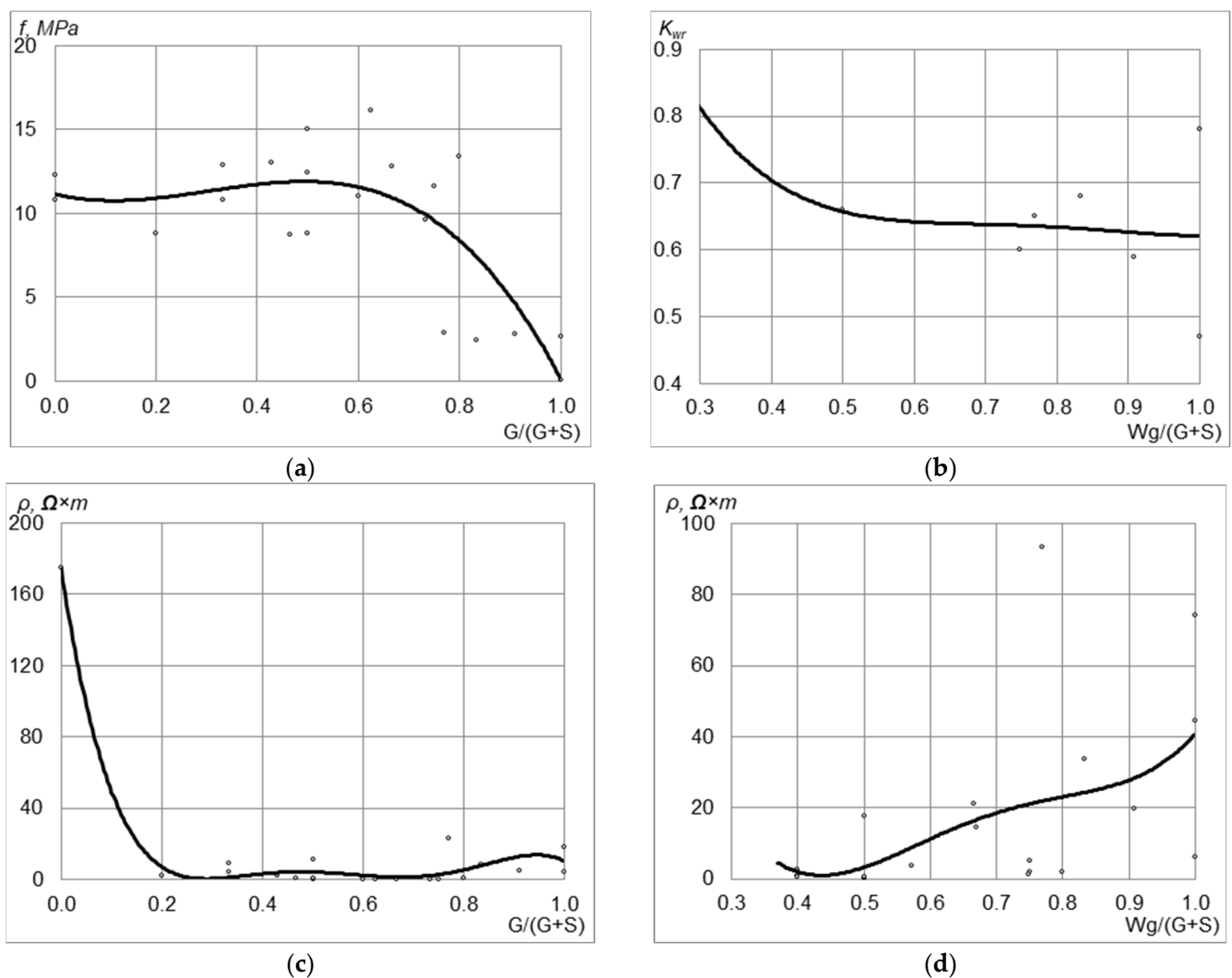


Figure 3. The effect of relative content of graphite filler $G/(G + S)$ and sodium silicate $Wg/(G + S)$ on compressive strength f (a), coefficient of water resistance (softening) K_{wr} (b) and electrical resistivity ρ (c,d) of the composite.

The compressive strength of the composite f exceeded 10 MPa, and the K_{wr} was not less than 0.6 with a graphite content in the total amount of filler $G/(G + S)$ of about 0.7 (Figure 3a). However, the water resistance of the composite was determined to the greatest extent by the liquid–solid ratio $Wg/(G + S)$. The maximum values of the water resistance coefficient K_{wr} , reaching 0.8, were observed at $Wg/(G + S) = 0.3–0.4$ (Figure 3b). The

minimum values of electrical resistivity, up to $1\text{--}0.3 \Omega \times \text{m}$, were observed at a relative content of graphite filler $G/(G + S)$ within $0.2\text{--}0.8$ (Figure 3c) and a liquid–solid ratio—relative content of sodium silicate $W_g/(G + S)$ —within $0.4\text{--}0.6$ (Figure 3d). In a composite that contains only graphite powder as a filler, shrinkage cracks form during hardening. The introduction of ground blast-furnace granulated slag in an amount of at least 0.1 of the amount of sodium silicate prevented the formation of shrinkage cracks. Humidification and water saturation of the silicate composite caused a decrease in its electrical resistivity, reaching a minimum value after 1 h of contact with water.

In order to study the interaction of the components of the composite, physicochemical studies were performed. Figure 4 shows the IR absorption spectra of sodium silicate cured with sodium fluorosilicate without additives and with the addition of sulfonated naphthalene formaldehyde, slag and graphite.

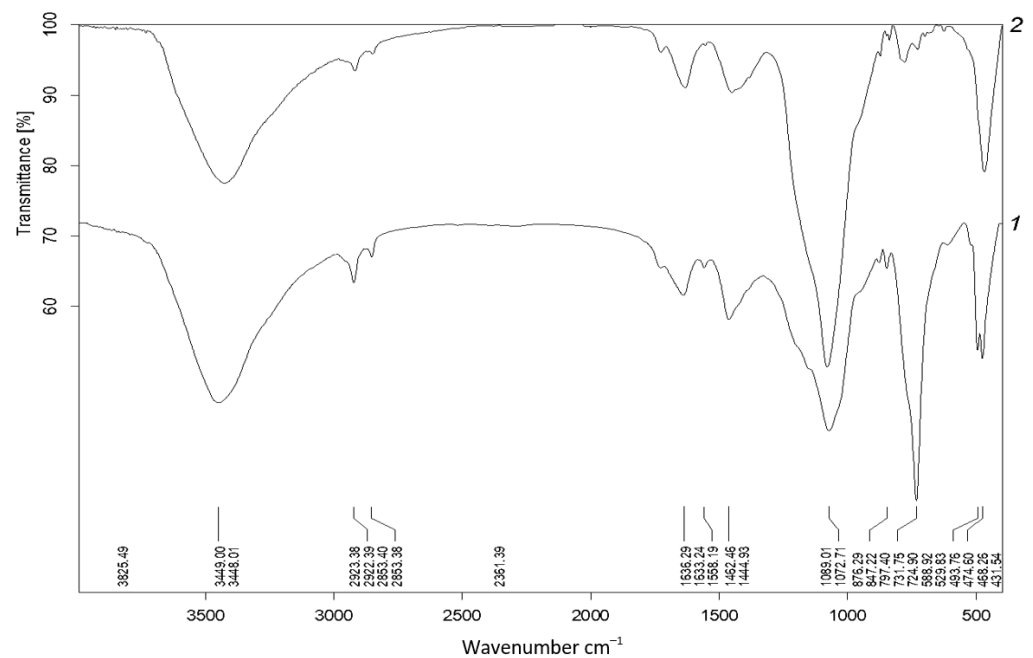


Figure 4. IR spectra of sodium silicate cured with sodium fluorosilicate without additives (1) and with additives of sulfonated naphthalene formaldehyde, slag and graphite (2).

For sodium silicate with a hardener, the following absorption bands were characteristic: $3200\text{--}3500$ and 1635 cm^{-1} —molecular water; $2700\text{--}3000 \text{ cm}^{-1}$ —hydrogen bonding; $1450\text{--}1460 \text{ cm}^{-1}$ —carbonate band vibrations; $1000\text{--}1200 \text{ cm}^{-1}$ —bond stretching vibrations Si–O; 770 cm^{-1} —Si–O–Si symmetrical stretching of bridging oxygens between tetrahedra; $460\text{--}480 \text{ cm}^{-1}$ —deformation vibrations of the bond Si–O–Si. The high intensity of the band at 1100 cm^{-1} , which corresponded to vibrations of the O–H bond in the Si–O–H groups, was apparently due to the polycondensation of HSiO_4^{3-} , H_3SiO_4^- and $\text{H}_4\text{SiO}_4^{aq}$ ions. Sodium silicate, approved by silicon-sodium fluoride, contained only condensed silicic tetrahedra (no band $900\text{--}1000 \text{ cm}^{-1}$), but together with silicic acid can contain fluorides ($400\text{--}600 \text{ cm}^{-1}$) and silicon-fluoride ($600\text{--}950 \text{ cm}^{-1}$).

The following changes occurred in IR spectra of sodium silicate cured with sodium fluorosilicate and with additives of sulfonated naphthalene formaldehyde, slag and graphite: the intensity of the band at 730 cm^{-1} decreased significantly; the band at 493 cm^{-1} disappeared; and the band at 780 cm^{-1} appeared, which indicates the presence of the $[\text{AlO}_4]^{-4}$ group. An increase in intensity and a shift towards higher wavenumbers of the $1000\text{--}1100 \text{ cm}^{-1}$ band were also observed.

Figure 5 shows X-ray diffraction patterns of the respective composites. The X-ray diffraction pattern of sodium silicate cured with sodium silicon fluoride contained several distinct diffraction peaks, the combination of which suggests the presence of a significant

amount of sodium fluoride (2.30 Å) and a small amount of sodium silicon fluoride (2.31; 3.31; 4.40 Å) and quartz (1.8; 2.27; 3.31 Å). Sodium silicon fluoride was the remainder of the original component; fragments of quartz-like structures could be formed as a result of the condensation of silicic acid. On the X-ray diffraction patterns of the composite containing graphite, diffraction maxima appeared 3.18–3.19; 3.24; 6.35–6.38; 6.47–6.48; 7.1 Å. Since they are typical for graphite, this confirms the hypothesis that there is no chemical interaction of graphite with sodium silicate and other components of the composite.

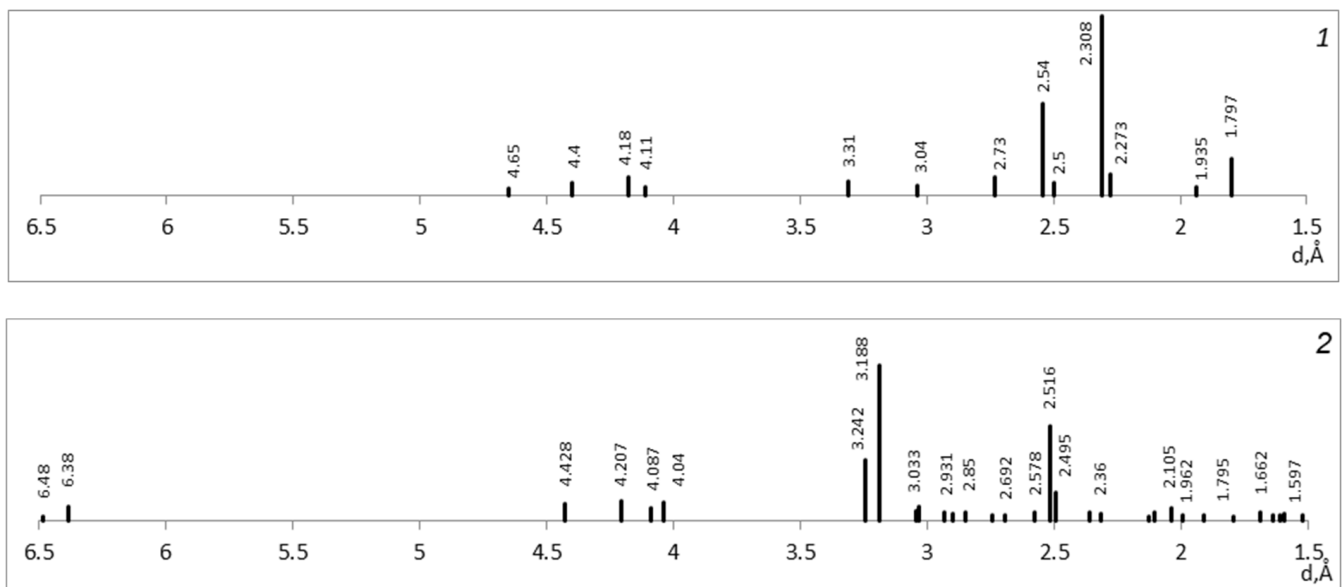


Figure 5. X-ray bar graphs of sodium silicate cured with sodium fluorosilicate without additives (1) and with additives of sulfonated naphthalene formaldehyde, slag and graphite (2).

Analysis of the IR spectra and X-ray patterns generally confirmed the notion that sodium silicate cured with sodium fluorosilicate contains silicic acid gel and sodium fluoride. Sodium silicate, cured with sodium fluorosilicate with the addition of granulated blast-furnace slag, contains silicic acid, calcium and sodium hydroaluminosilicates and calcium hydrosilicates, but does not contain sodium fluoride. At the same time, calcium and sodium hydroaluminosilicates are contained less than in a composite of slag cured with sodium silicate (slag–alkali binder). The chemical interaction of graphite with sodium silicate and other components of the composite by physicochemical methods was not revealed. Therefore, graphite remained in an unbound state and retained electrical conductivity.

Figure 6 shows the data of scanning electron microscopy with X-ray microanalysis. Analysis of Figure 6 shows that the surfaces of the cleavages of the composite are porous and rough, the graphite particles on the pictures are gray in color and have an amorphous structure, similar to the grains of metals (iron, chromium, titanium). However, graphite is difficult to identify because its surface is covered with small particles of the reaction products of sodium silicate and sodium silicon fluoride. It can be seen from the pictures that the structure of sodium silicate, cured with sodium silicon fluoride and with the addition of graphite, is dispersed, consists of gel-like formations and crystalline particles ranging in size from less than 1 micron to several microns, as well as inclusions of larger particles ranging in size from tens of microns to 100 microns. A joint analysis of the electron microscopic image and the X-ray surface map showed that sodium silicate cured with sodium fluorosilicate, with the addition of graphite, has the structure of a composite material with a filler of particles of graphite C (29%–33% of the surface) distributed over the volume. The composite matrix consists of the products of the interaction of sodium silicate and sodium fluorosilicate and includes elements such as O (45%–50%), Si (8%–11%), F (4%–5%), Na (1.4%), Al (1.2%–2%), Ca (0.9%–1.9%), etc. (less than 1% each), which are

evenly distributed. It has been confirmed that due to the interaction of sodium silicate and sodium fluorosilicate, new products of predominantly gel-like structure are formed. There is no chemical interaction of sodium silicate and sodium fluorosilicate with graphite; graphite remains in an unbound state and retains electrical conductivity.

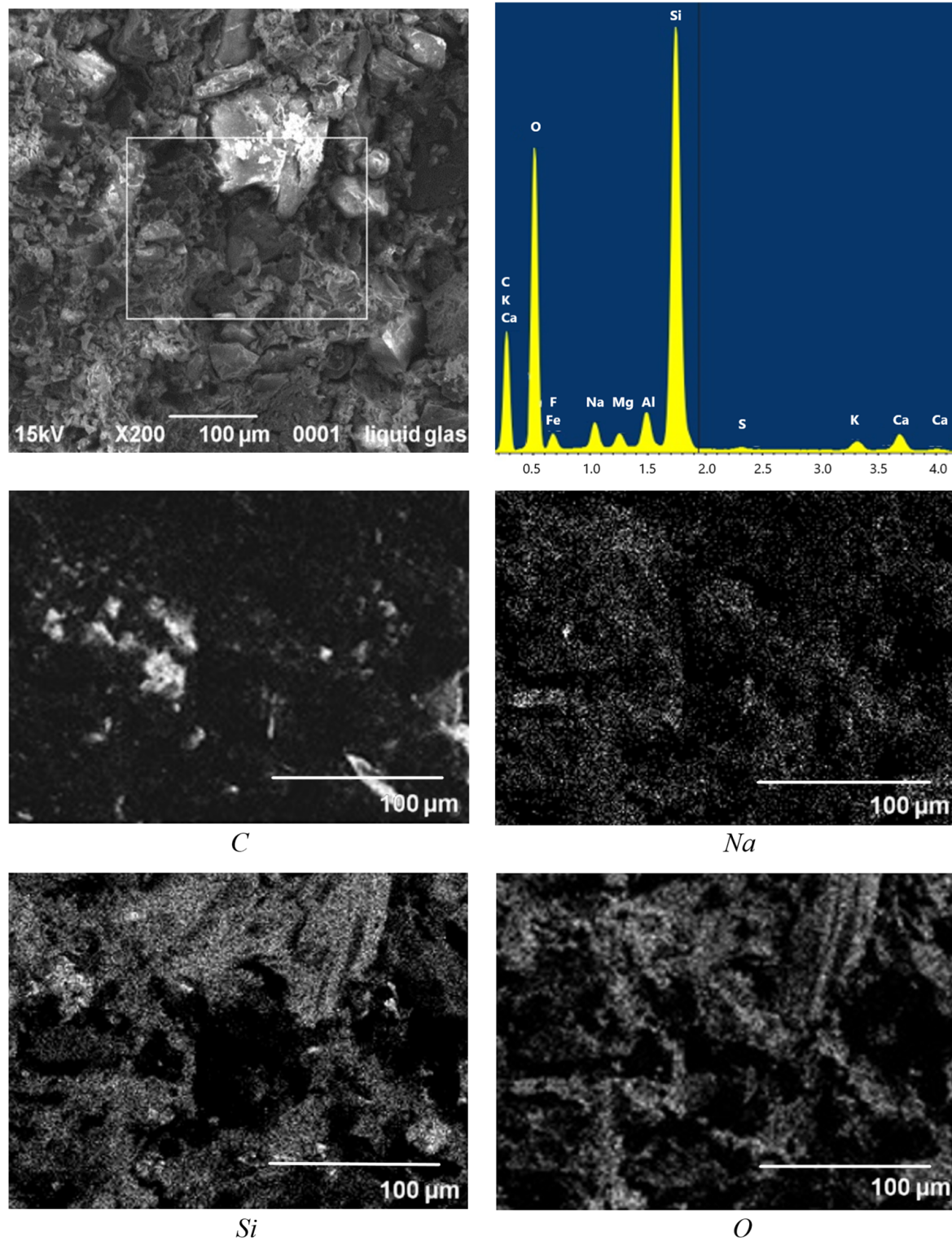


Figure 6. Electron microscopic images ($\times 200$) and X-ray maps of the distribution of elements on the surface of sodium silicate, cured by sodium fluorosilicate, with the addition of graphite.

5. Discussion

We theoretically substantiated the creation of electrically conductive silicate composites for protection against the electrocorrosion of structures. An increase in water resistance was provided by the formation of insoluble zeolite-like sodium and calcium aluminosilicates.

The products of the interaction between silicate and sodium silicic fluoride are orthosilicic acid gel Si(OH)_4 and sodium fluoride NaF, the particles of which have a negative surface charge and form non-water resistant electro-homogeneous contacts with each other. In the case of adding ground blast-furnace granulated slag, its compounds interact with NaF to form alkaline and alkaline earth hydroaluminosilicates, hydroaluminate C_3AH_6 and calcium fluoride CaF_2 . C_3AH_6 and CaF_2 particles have a positive surface charge and form electro-heterogeneous contacts with Si(OH)_4 , which provide an increase in the water resistance of the composite. Thermodynamic calculations were performed to establish the possibility of the formation of hydronepheline NAS_2H_2 , calcium hydroaluminate C_3AH_6 and calcium fluoride CaF_2 due to the interaction of slag with sodium fluoride NaF.

It has been experimentally established that the electrophysical properties of the composite are in antagonism with the physico-mechanical and hydrophysical ones; therefore, the development of its composite should be carried out using methods of compromise optimization. The specific electrical resistance of the composite r depends on the content of graphite $G/(G + S)$ and sodium silicate $Wg/(G + S)$; the minimum $r = 0.2\text{--}1 \Omega \times \text{m}$ is observed for $G/(G + S) = 0.2\text{--}0.8$ and $CH/(G + S) = 0.4\text{--}0.9$. The water resistance of K_{wr} depends mainly on $Wg/(G + W)$ and is maximum (up to 0.8) at $Wg/(G + W) = 0.3\text{--}1.0$ and $G/(G + W)$ close to 0.7. In a composite that contains only graphite as a filler, shrinkage cracks are formed. The introduction of slag in an amount of at least 0.1 of sodium silicate prevents their formation.

As a result of physical and chemical studies, it was confirmed that the products of the interaction of silicate and sodium fluorosilicate are Si(OH)_4 and NaF, and with the addition of slag, the products are Si(OH)_4 , calcium and sodium hydroaluminosilicates and calcium hydrosilicates. As a result of electron microscopic studies, it was found that the composite has the structure of a matrix composite with a filler of uniformly distributed graphite and a matrix of hardening products with a predominantly gel-like structure. The chemical interaction of graphite with the components of the composite was not found; therefore, graphite remained in an unbound state and retained electrical conductivity.

Author Contributions: Conceptualization, A.P. and O.B.; methodology, A.P., T.R. and O.B.; formal analysis, T.R. and O.P.; investigation, O.B., O.P. and V.Z.; resources, O.P. and V.Z.; writing—original draft preparation, O.B. and O.P.; writing—review and editing, A.P., T.R. and O.B.; visualization, O.B. and V.Z. All authors have read and agreed to the published version of the manuscript.

Funding: This research received no external funding.

Data Availability Statement: The data presented in this study are available upon reasonable request from the corresponding author.

Conflicts of Interest: The authors declare no conflict of interest.

References

1. Plugin, D.; Kasyanov, V.; Konev, V.; Nesterenko, S.; Afanasiev, A. Research into the effectiveness of grounded screens of electroconductive silicate compositions for electrocorrosion protection. *MATEC Web Conf.* **2017**, *116*, 1012. [[CrossRef](#)]
2. Plugin, A.A.; Pluhin, O.A.; Kasyanov, V.V.; Dyomina, O.I.; Bondarenko, D.O. Portland cement-based penetrating electrically conductive composition for protection against electrocorrosion. *Funct. Mater.* **2021**, *28*, 121–130. [[CrossRef](#)]
3. Koniev, V. Electrically Conductive Silicate Composition for Protection against Electrocorrosion of Railway Structures. Ph.D. Thesis, Ukrainian State University of Railway Transport, Kharkiv, Ukraine, 2021.
4. Ding, Y.; Chen, Z.; Han, Z.; Zhang, Y.; Pacheco-Torgal, F. Nano-carbon black and carbon fiber as conductive materials for the diagnosing of the damage of concrete beam. *Constr. Build. Mater.* **2013**, *43*, 233–241. [[CrossRef](#)]
5. Baeza, J.; Galao, O.; Zornoza, E.; Garcés, P. Multifunctional Cement Composites Strain and Damage Sensors Applied on Reinforced Concrete (RC) Structural Elements Francisco. *Materials* **2013**, *6*, 841–855. [[CrossRef](#)] [[PubMed](#)]

6. Dinesha, A.; Sujib, D.; Pichumani, M. Electro-mechanical investigations of steel fiber reinforced self-sensing cement composite and their implications for real-time structural health monitoring. *J. Build. Eng.* **2022**, *511*, 104343. [CrossRef]
7. Yehia, S.; Tuan, C.Y.; Ferdon, D.; Chen, B. Conductive Concrete Overlay for Bridge Deck Deicing: Mixture Proportioning, Optimization, and Properties. *Mater. J.* **2000**, *97*, 172–181. [CrossRef]
8. Sassani, A.; Ceylan, H.; Kim, S.; Gopalakrishnan, K.; Arabzadeh, A.; Taylor, C.P. Factorial Study on Electrically Conductive Concrete Mix Design for Heated Pavement Systems. In Proceedings of the Transportation Research Board 96th Annual Meeting, Washington, DC, USA, 8–12 January 2017; Available online: <https://dr.lib.iastate.edu/handle/20.500.12876/13676> (accessed on 1 January 2017).
9. Khalid, T.; Albasha, L.; Qaddoumi, N.; Yehia, S. Feasibility Study of Using Electrically Conductive Concrete for Electromagnetic Shielding Applications as a Substitute for Carbon-Laced Polyurethane Absorbers in Anechoic Chambers. *IEEE Trans. Antennas Propag.* **2017**, *65*, 2428–2435. [CrossRef]
10. Carmona, J.; Garcés, P.; Climent, M.A. Efficiency of a conductive cement-based anodic system for the application of cathodic protection, cathodic prevention and electrochemical chloride extraction to control corrosion in reinforced concrete structures. *Corros. Sci.* **2015**, *96*, 102–111. [CrossRef]
11. Anwar, M.S.; Sujitha, B.; Vedalakshmi, R. Light-weight cementitious conductive anode for impressed current cathodic protection of steel reinforced concrete application. *Constr. Build. Mater.* **2014**, *71*, 167–180. [CrossRef]
12. Sassani, A.; Ceylan, H.; Kim, S.; Gopalakrishnan, K.; Arabzadeh, A.; Taylor, P.C. Influence of mix design variables on engineering properties of carbon fiber-modified electrically conductive concrete. *Constr. Build. Mater.* **2017**, *152*, 168–181. [CrossRef]
13. García-Macías, E.; D’Alessandro, A.; Castro-Triguero, R.; Pérez-Mira, D.; Ubertini, F. Micromechanics modeling of the electrical conductivity of carbon nanotube cement-matrix composites. *Compos. Part B Eng.* **2017**, *108*, 451–469. [CrossRef]
14. Jang, D.; Yoon, H.N.; Yang, B.; Seo, J.; Farooq, S.Z.; Lee, H.K. Synergistic effects of CNT and CB inclusion on the piezoresistive sensing behaviors of cementitious composites blended with fly ash. *Smart Struct. Syst.* **2022**, *29*, 351–359. [CrossRef]
15. Fiala, L.; Petříková, M.; Černý, R. Electrical properties and self-heating ability of alkaliactivated slag with graphite powder. *Green Build. Technol. Mater.* **2020**, *20*, 359–366. [CrossRef]
16. Fiala, L.; Petříková, M.; Lin, W.-T.; Podolka, L.; Černý, R. Self-Heating Ability of Geopolymers Enhanced by Carbon Black Admixtures at Different Voltage Loads. *Energies* **2019**, *12*, 4121. [CrossRef]
17. Černý, Z.; Jakubec, I.; Bezdička, P.; Šulc, L.; Macháček, J.; Bludská, J.; Roubíček, P. Preparation of electrically conductive materials based on geopolymers with graphite. *Ceram. Eng. Sci. Proc.* **2010**, *31*, 91–99.
18. Wang, D.; Wang, Q.; Huang, Z. Investigation on the poor fluidity of electrically conductive cement-graphite paste: Experiment and simulation. *Mater. Des.* **2019**, *169*, 107679. [CrossRef]
19. Łach, M.; Hebdowska-Krupa, M.; Mierzwiński, D.; Korniejenko, K. Mechanical properties of geopolymers reinforced with carbon and aramid long fibers. *IOP Conf. Ser. Mater. Sci. Eng.* **2019**, *706*, 012011. [CrossRef]
20. Zmeskal, O.; Trhlikova, L.; Pospisil, J.; Fiala, L.; Florian, P. Investigation of electric and thermal properties of alkali-activated aluminosilicates with a cnt admixture. *Ceram. Silikáty* **2020**, *64*, 180–189. [CrossRef]
21. Babushkin, V.I.; Plugin, A.A.; Zelensky, D.Y. Thermodynamic and physico-chemical studies of acid-resistant binders based on water glass and sodium silicon fluoride. *Collect. Sci. Work. Ukr. State Univ. Railw. Transp.* **2000**, *37*, 55–62.
22. Palomo, A.; Krivenko, P.; Garcia-Lodeiro, I.; Kavalerova, E.; Maltseva, O.; Fernández-Jiménez, A. A review on alkaline activation: New analytical perspectives. *Mater. Constr.* **2014**, *64*, e022. [CrossRef]
23. Krivenko, P. Why alkaline activation—60 years of the theory and practice of alkali-activated materials. *J. Ceram. Sci. Technol.* **2017**, *8*, 323–333. [CrossRef]
24. Babushkin, V.I.; Matveyev, G.M.; Mchedlov-Petrossyan, O.P. *Thermodynamics of Silicates; Original Russian edition published by Stroissdat, Moscow; Edycja Softcover Reprint of the Original*, 1st ed.; Springer: Berlin/Heidelberg, Germany, 1985; 475p.
25. Ovcharenko, F.D.; Arkhipov, V.V.; Biryukov, A.I.; Plugin, A.N. Electro-surface phenomena and the evaluation of processes in the ardening of mineral binders and concretes prepared from these binders. *Colloid J. USSR* **1981**, *43*, 713–717. Available online: <https://www.webofscience.com/wos/woscc/full-record/WOS:A1981NR37500007> (accessed on 1 January 1981).
26. Plugin, A.N.; Vdovenko, N.V.; Biriukov, A.I.; Ovcharenko, F.D. On the mechanism of advent of the electro-surface potential of different substances in aqueous-solutions. *Dokl. Akad. Nauk SSSR* **1988**, *298*, 656–661. Available online: <https://www.webofscience.com/wos/woscc/full-record/WOS:A1988M134500036> (accessed on 1 January 1988).
27. Plugin, A.N.; Plugin, A.A.; Trykoz, L.V. *Fundamentals of the Theory of Hardening, Strength, Destruction and Durability of Portland Cement, Concrete and Structures Made of Them. 1 Colloidal Chemistry and Physical-Chemical Mechanics of Cement Concrete*; Naukova Dumka: Kyiv, Ukraine, 2011; 331p.
28. Bergna, H.E. Chapter 1. Advances in Chemistry. In *The Colloid Chemistry of Silica*; Bergna, H.E., Ed.; American Chemical Society: Washington, DC, USA, 1994; Volume 234, pp. 1–47. [CrossRef]
29. Ren, Z.; Sun, J.; Tang, W.; Zeng, X.; Zeng, H.; Wang, Y.; Wang, X. Mechanical and electrical properties investigation for electrically conductive cementitious composite containing nano-graphite activated magnetite. *J. Build. Eng.* **2022**, *57*, 104847. [CrossRef]
30. Gopalakrishnan, K.; Ceylan, H.; Kim, S.; Yang, S.; Abdulla, H. Electrically Conductive Mortar Characterization for Self-Heating Airfield Concrete Pavement Mix Design. *Int. J. Pavement Res. Technol.* **2015**, *8*, 315–324. [CrossRef]
31. Pluhin, O.; Plugin, A.; Plugin, D.; Borziak, O.; Dudin, O. The effect of structural characteristics on electrical and physical properties of electrically conductive compositions based on mineral binders. *MATEC Web Conf.* **2017**, *116*, 01013. [CrossRef]

32. Ahmed, S.; Kamal, I. Green Conductive Construction Materials toward Sustainable Infrastructures. *ECS Trans.* **2022**, *107*, 2139. [[CrossRef](#)]
33. Fraç, M.; Szudek, W.; Szoldra, P.; Pichór, W. The applicability of shungite as an electrically conductive additive in cement composites. *J. Build. Eng.* **2022**, *45*, 103469. [[CrossRef](#)]
34. Majerová, J.; Drochytka, R. Possibilities of utilization of waste materials in production of electrically conductive composites on silicate basis. *Solid State Phenom.* **2021**, *321*, 171–176. [[CrossRef](#)]

Disclaimer/Publisher's Note: The statements, opinions and data contained in all publications are solely those of the individual author(s) and contributor(s) and not of MDPI and/or the editor(s). MDPI and/or the editor(s) disclaim responsibility for any injury to people or property resulting from any ideas, methods, instructions or products referred to in the content.